ANL/CMT/CP-95570

IMAGING DIFFUSION WITH NON-CONSTANT B_1 GRADIENTS*

Klaus Woelk, Bernd L.J. Zwank, and Joachim Bargon
Institut für Physikalische und Theoretische Chemie, Universitat Bonn
Wegelerstr. 12, D-53115 Bonn, Germany

Robert J. Klingler, Rex E. Gerald II, and Jerome W. Rathke
Chemical Technology Division, Argonne National Laboratory
9700 South Cass Avenue, Argonne, Illinois 60439 USA

For publication in "Spatially Resolved Magnetic Resonance"

January 1998

* Work supported by the U.S. Department of Energy, Division of Chemical Sciences, Office of Basic Energy Sciences, under Contract W-31-109-ENG-38 and by the German Research Foundation (DFG) under Program Wo 613/2-1.

DISCLAIMER

X. Imaging Diffusion With Non-constant B_1 Gradients

Klaus Woelk, Bernd L. J. Zwank, and Joachim Bargon
Institut für Physikalische und Theoretische Chemie, Universität Bonn
Wegelerstr. 12, D-53115 Bonn, Germany

Robert J. Klingler, Rex E. Gerald II, and Jerome W. Rathke
Chemical Technology Division, Argonne National Laboratory
9700 South Cass Avenue, Argonne, Illinois 60439, USA

woelk@rs1.thch.uni-bonn.de

Rotating-frame imaging with the mathematically well-defined, non-constant magnetic field gradient of toroid cavity detectors represents a new technique to evaluate diffusion in solids, fluids or mixed-phase systems. While conventional NMR methods to measure diffusion utilize constant magnetic field gradients and, therefore, constant k-space wave numbers across the sample volume, the hyperbolic B_1 fields of toroid cavity detectors exhibit large ranges of wave numbers radially distributed around the central conductor. As a consequence, signal amplitudes decay depending on the radial distance from the center axis of the torus. Applying a numerical finite-difference procedure to solve partial differential transport equations makes it possible not only to determine diffusion in toroid detectors to a high precision but also to include and accurately reproduce transport phenomena at or through singularities, such as phase transitions, membranes or impermeable boundaries.

X.1 Introduction

The *diffusion* measurements introduced here are based on *rotating-frame imaging* (RFI), i.e., B_1-gradient imaging, first introduced by Hoult [1]. In rotating-frame imaging, spatial resolution is obtained from NMR spectra with incrementally increasing pulse widths. After a two-dimensional Fourier transformation, nutation frequencies of NMR-active nuclei are derived versus chemical shift. Since nutation frequencies are proportional to the B_1 field at the location of a nucleus, a transformation into spatial information is easily conducted if the B_1 field distribution is known. More recent rotating-frame imaging applications utilize the time-saving, chemical-shift selective *rapid-imaging pulse train* (RIPT) [2-4], where a one-dimensional, real Fourier transformation reveals an image of nuclei precessing at the transmitter frequency.

A quantitative image of spin density versus distance is revealed [5], when signal-intensities are corrected under consideration of the sample volume and the principle of reciprocity [6].

X.1.1 Magnetization-Grating Rotating-Frame Imaging

To extract diffusion coefficients of fluids, Kimmich et al. [7] introduced *magnetization-grating rotating-frame imaging* (MAGROFI) that employs constant B_1 gradients of *surface coils* to create homogeneous *z-magnetization gratings* across a sample. The gratings are generated by single hard pulses (preparation pulse, P1 in Fig. X.1) applied with the same constant gradient that is later used for recording the image (P2 in Fig. X.1). During an evolution time τ between the preparation pulse and the imaging procedure, the initial grating decays because of T_1 *relaxation* and diffusion.

If the evolution time is shorter than five times T_2, undesired transversal magnetization remains from the preparation pulse. This part of the magnetization is usually removed by putting the pulse sequence through a transmitter *phase cycling* of the preparation pulse versus the imaging pulses. The remaining z-grating is sampled by RFI and analyzed to extract the *diffusion coefficient*.

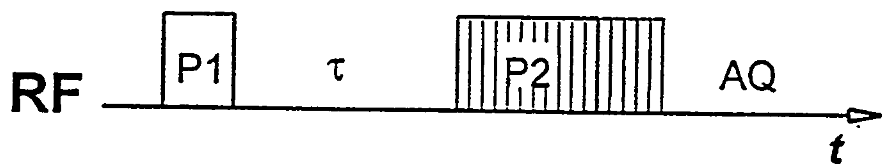

Fig. X.1: Pulse sequence of the MAGROFI experiment. In a B_1 gradient, the preparation pulse P1 generates a z-magnetization grating that, after an evolution period τ, is imaged by the rotating frame imaging procedure P2.

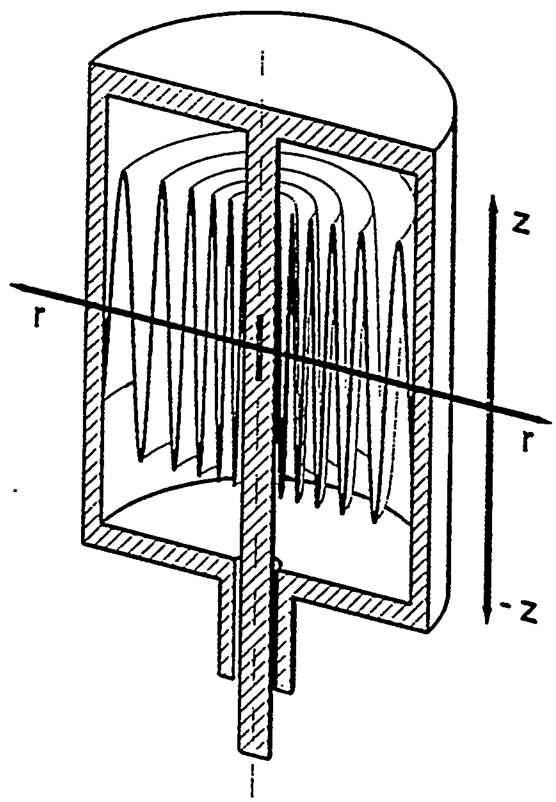

Fig. X.2: Schematic drawing of a toroid cavity detector used for diffusion measurements with the MAGROFI technique. The detector consists of a central conductor and a cilindrical hollow body. The sensitive volume is confined to the inside of the torus. Inside the detector, a z-magnetization grating generated by a single hard pulse P1 is shown.

Unfortunately, a single surface-coil MAGROFI experiment delivers only one data point for a linear regression of amplitudes versus evolution time [7] or, alternatively, versus *k*-space wave number. Accordingly, many MAGROFI experiments with different evolution times or different preparation pulse width, respectively, must be recorded to determine a single diffusion coefficient.

X.1.2 Imaging Diffusion in Toroid Cavity Detectors

The MAGROFI experiment can also be applied to the non-constant gradients of coaxial *toroid cavity detectors* (Fig. X.2) [8].

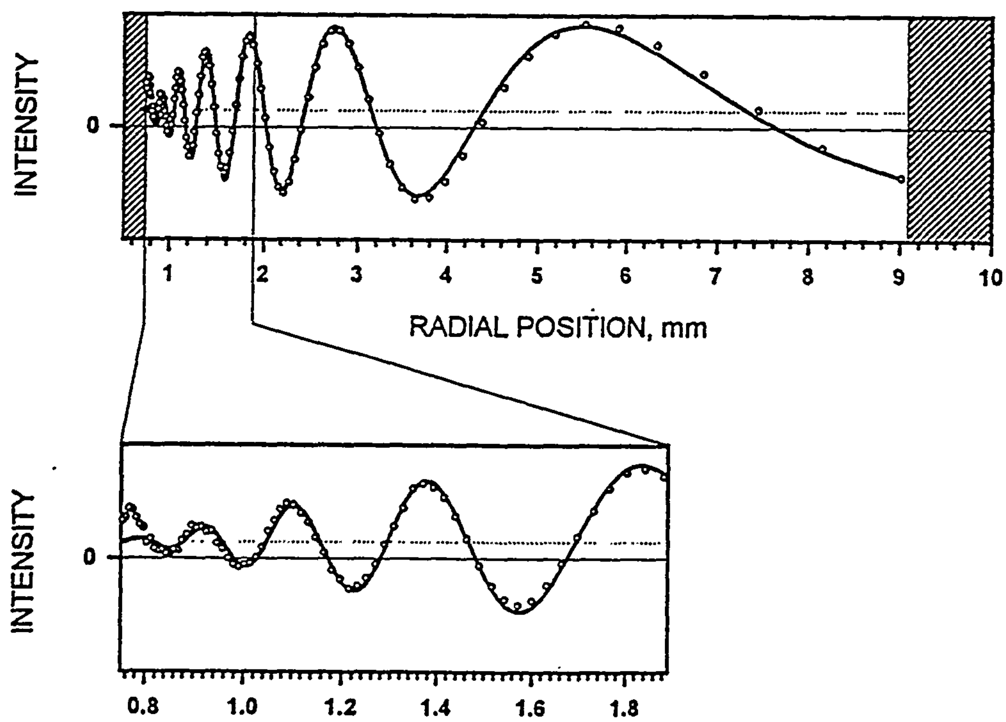

Fig. X.3: MAGROFI experiment in a toroid cavity detector. The wave number of the asymmetric magnetization grating is large near the central conductor and drops of with increasing radial distance. Experimental data (hollow circles) from a chloroform solution are compared to the analysis based on analytical propagation equations (solid line). Diffusive edge enhancement is visible at the central conductor (lower detailed plot).

However, as a consequence of the hyperbolic B_1 field of toroids ($B_1 = A/r$, where A is a proportionality constant (torus factor), and r is the radial distance from the long axis of the torus), the wave number of the grating changes continuously with the radius. Diffusion causes a fast decay of the grating, where the wave number is high, and a slow decay, where it is small (Fig. X.3). In contrast, the form of the grating, either symmetric or asymmetric, does not effect T_1 relaxation that uniformly returns z-magnetization to Boltzmann equilibrium. Because of the large range of wave numbers exhibited in toroid detectors, a single RFI experiment is sufficient to extract diffusion coefficients from three-parameter computer fits of *propagation equations* [8], refining T_1, D, and I (i.e., longitudinal relaxation time, diffusion coefficient and signal amplitude, respectively). Additionally, because B_1 gradients in toroid cavity detectors are very "clean", i.e., mathematically well-defined, and very strong, diffusion coefficients are extracted to a high precision.

X.2 Partial Differential Transport Equations

Fick's first and second law of diffusion are basic *partial differential equations* to analyze isotropic transport of matter because of *Brownian motion.* For z-magnetization gratings generated by MAGROFI experiments, Fick's equations can be solved analytically if the gradient is strictly constant, the sample expands evenly perpendicular to the gradient, and contains no *singularities* along the gradient. Furthermore, the diffusion coefficient must be independent of concentration and space. Therefore, the analysis of experimental data with analytical solutions is limited to homogeneous samples remote from the walls of the sample container. Phenomena that occur at singularities, such as phase transitions, membranes or impermeable boundaries (e.g. *diffusive edge enhancement* [9], Fig. X.3), must be analyzed by numerical approaches.

The decay of magnetization by diffusion represents a *open-ended propagation problem* that starts with an initial condition, i.e., the initial grating generated by the preparation pulse. Additionally, impermeable boundaries (the walls of the sample container) or other known singularities confine the spacial range of analysis.

X.2.1 Finite-Difference Approach

If the time progress of a functionality with complex boundary conditions cannot be followed with analytical equations, *finite-difference calculations* are commonly used to numerically solve propagation problems [10]. In a finite-difference procedure, data points of an initial condition are repeatedly advanced by finite time steps until the experimental data set is matched to a maximum likelihood. Thereafter, the transport parameter or functionality is evaluated from the number and width of time steps.

Applying Finite-Differences to Magnetization Gratings

To analyze MAGROFI experiments with finite differences in time and space, every experimental data location is progressed by finite time steps starting from the initial grating. For each location, the change of magnetization density is estimated by solving the parabolic partial differential equation $\partial c/\partial t = \partial(D\partial c)/\partial x^2$, where c is the magnetization density, and x is the spatial dimension along the B_1 gradient. *Concentration-dependence of the diffusion coefficient*, the shape of the sample volume, or singularities can all be included into the parabolic differential equation. For example, data points remote from singularities need the magnetization densities of the two neighboring data locations as boundary conditions. For points adjacent to singularities, however, a boundary condition such as the impermeability of the sample container applies.

The maximum time step (Δt) that can be used without the numerical solution diverge from the true solution is given by the *Einstein-Smoluchowski relation* [11], which determines the mean square distance a particle travels by random walk (i.e., $\Delta x^2 = 2D\Delta t$). The distance Δx must not be larger than the smallest interval between two data points. Otherwise particles would travel further than from one data-point location to the next. As a consequence, data points further apart than the neighboring data must be included as boundary conditions and higher-order partial differential equations must be solved. The relation that limits the time step of finite-difference procedures is generally known as *Courant's condition* [12].

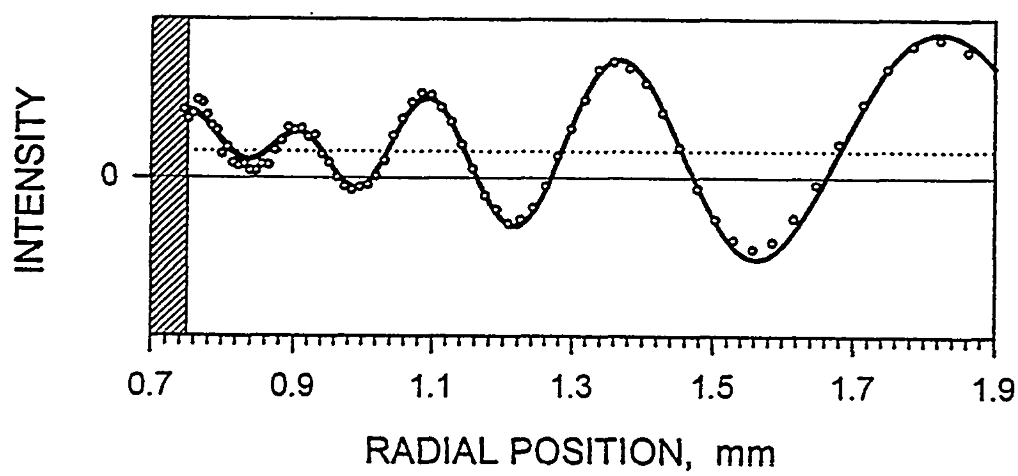

Fig. X.4: Finite-difference analysis of the diffusive edge enhancement at the central conductor of a toroid cavity. The numerical simulation (solid line) matches the experimental data (open circles) even at the impermeable singularity. A diffusion coefficient of $D = 2.16 \times 10^{-9}$ m^2 s^{-1} was found for the chloroform sample.

Fit to Experimental data

Fig. X.4 shows the finite-difference simulation that has been fitted to experimental data by a *least-squares optimization* refining T_1, D, and I. Clearly, the diffusive edge enhancement is accurately reproduced, while the analytical propagation equation can only be used to analyze data remote from singularities (Fig. X.3). In addition, the finite-difference solution reveals that, in toroid detectors, grating extrema tend to shift to smaller radii. This effect has been observed before [8] when grating extrema decayed down to less than 10% of their initial value but is not accounted for by analytical propagation equations.

X.3 Summary

The MAGROFI technique presents a robust and versatile method to evaluate diffusion. If applied with the non-constant, mathematically well-defined and strong gradient of toroid cavity detectors, it reveals an excellent tool to measure diffusion very precisely in a single rotating-frame imaging experiment. Since the normally derived, analytical propagation equations are limited to constant gradients and areas remote from singularities, a finite-difference numerical procedure is required to follow the effects of diffusion correctly. Furthermore, the numerical approach makes it possible to analyze diffusion in mixed-phase systems and through membranes or other singularities. As an example, diffusive edge enhancement observed adjacent to impermeable boundaries has been reproduced accurately by the numerical approach.

References

1. D. I. Hoult, *J. Magn. Reson.* **33**, 183 (1979).
2. K. R. Metz and J. P. Boehmer, *Magn. Reson. Imaging* **6** (Suppl. 1), 53 (1988).
3. J. L. Bowers, P. M. Macdonald, and K. R. Metz, *J. Magn. Reson. Ser. B* **106**, 72 (1994).
4. D. Canet, *Progr. NMR Spectr.* **30**, 101 (1997).
5. K. Woelk, J. W. Rathke, and R. J. Klingler, *J. Magn. Reson. A* **109**, 137 (1994).
6. D. I. Hoult and R. E. Richards, *J. Magn. Reson.* **24**, 71 (1976).
7. R. Kimmich, B. Simon, and H. Köstler, *J. Magn. Reson. A* **112**, 7 (1995).
8. K. Woelk, R. E. Gerald II, R. J. Klingler, and J. W. Rathke, *J. Magn. Reson. A* **121**,

74 (1996).

9. B. Pütz, D. Barsky, and K. Schulten, *Chem. Phys. Lett.* **183**, 391 (1991).
10. J. Crank, "The Mathematics of Diffusion," 2. Ed, p. 141, Oxford University Press, Oxford (1975).
11. P. W. Atkins, "Physical Chemistry," 3. Ed., p. 681, Oxford University Press, Oxford (1986).
12. R. Courant, K. Friedrichs, and H. Lewy, *Mathematische Annalen* **100**, 32 (1928).

Acknowledgements

This work was supported by the U.S. Department of Energy, Division of Chemical Sciences, Office of Basic Energy Sciences, under Contract W-31-109-Eng-38 and by the German Research Foundation (DFG) under program Wo 613/2-1. We thank Prof. Dr. G. Woelk, Technical University of Aachen, Germany for many helpful discussions.